Model-Based Control of FES-Induced Single Joint Movements

Maurizio Ferrarin, *Member, IEEE*, Francesco Palazzo, Robert Riener, *Member IEEE*, and Jochen Quintern

Abstract—A crucial issue of functional electrical stimulation (FES) is the control of motor function by the artificial activation of paralyzed muscles. Major problems that limit the success of current FES systems are the nonlinearity of the target system and the rapid change of muscle properties due to fatigue. In this study, four different strategies, including an adaptive algorithm, to control the movement of the freely swinging shank were developed on the basis of computer simulations and experimentally evaluated on two subjects with paraplegia due to a complete thoracic spinal cord injury. After developing a nonlinear, physiologically based model describing the dynamic behavior of the knee joint and muscles, an open-loop approach, a closed-loop approach, and a combination of both were tested. In order to automate the individual adjustments cited above, we further evaluated the performances of an adaptive feedforward controller. The two parameters chosen for the adaptation were the threshold pulse width and the scaling factor for adjusting the active moment produced by the stimulated muscle to the fitness of the muscle. These parameters have been chosen because of their significant time variability. The first three controllers with fixed parameters yielded satisfactory result. An additional improvement was achieved by applying the adaptive algorithm that could cope with problems due to muscle fatigue, thus permitting on-line identification of critical parameters of the plant. Although the present study is limited to a simplified experimental setup, its applicability to more complex and functional movements can be expected.

Index Terms—Adaptive control, biomechanical model, closed-loop control, functional electrical stimulation (FES), model-based control, rehabilitation engineering.

I. INTRODUCTION

CONTROLLING movements of paralyzed limbs in spinal cord injured subjects by means of functional electrical stimulation (FES) is a particularly complex problem. Difficulties arise from the plant being a nonlinear, highly time-varying and, in case of antigravitational motor tasks, unstable system. The design of control strategies can greatly benefit from a model-based approach; in principle, better muscle models mean better control.

Many control methods have been tested and reported in the literature; both feedforward [1], [2] and feedback controllers

[3]–[6] have been examined, whose performance depends mainly on the model accuracy in the first case and on the tuning of the controller parameters in the second case. In some studies also the combination of feedforward and feedback components has been proposed [7], [8] in order to exploit optimally their specific performances. In particular, Chang *et al.* [8] compared a feedforward neuro-controller, a proportional integrative derivative (PID) controller and their combination (neuro-PID controller). In that study the feedforward component was realized with a multilayer feedforward time-delay neural network, trained with signals obtained from experiments using lowpass filtered random sequence and initialized with the Nguyen–Widrow method. The experimental part of Chang's study was performed on one paraplegic patient in an experimental setup very similar to that adopted in the present paper; knee angle tracking tests during quadriceps stimulation on the freely swinging shank. The results showed that the neuro-PID controller demonstrated a slightly better performance than the neural controller alone and that the performances of the neural controller alone and the neuro-PID controller were significantly better than that of the PID controller.

Not many authors, however, have suggested an extensive use of nonlinear physiologically based models [9]. Moreover, open-loop controllers having fixed parameters are likely to fail, if physiological internal disturbances (such as fatigue-induced changes in the contractile properties of the motor units) affect the muscle dynamics. For this reason some studies have focused on FES adaptive controllers, able to cope with such time-varying phenomena. Bernotas *et al.* [10], for example, developed a discrete-time adaptive strategy to control the isometric contraction of cat muscles, while Hatwell *et al.* [11] implemented and tested a model reference adaptive controller (MRAC) on a patient finding, however, serious problems, mainly for the presence of the nonlinear recruitment characteristic. More recently, Riess *et al.* [12], [13] have evaluated under isotonic conditions an adaptive feedforward control algorithm utilizing neural network [pattern generator–pattern shaper (PG/PS) controller] and compared its performance with that of a standard PD feedback controller. Computer simulation and experimental results indicated that the PG/PS controller was able to achieve and maintain better tracking performance than the PD controller [12] and that this behavior is not much sensitive to the control system parameter values [13].

The main goal of the present study was to compare both in simulation and experimentally different control strategies. Compared to the last mentioned studies, which proposed a neural network control approach, we adopted a model closely based on the physiological processes underlying excitation and activation of
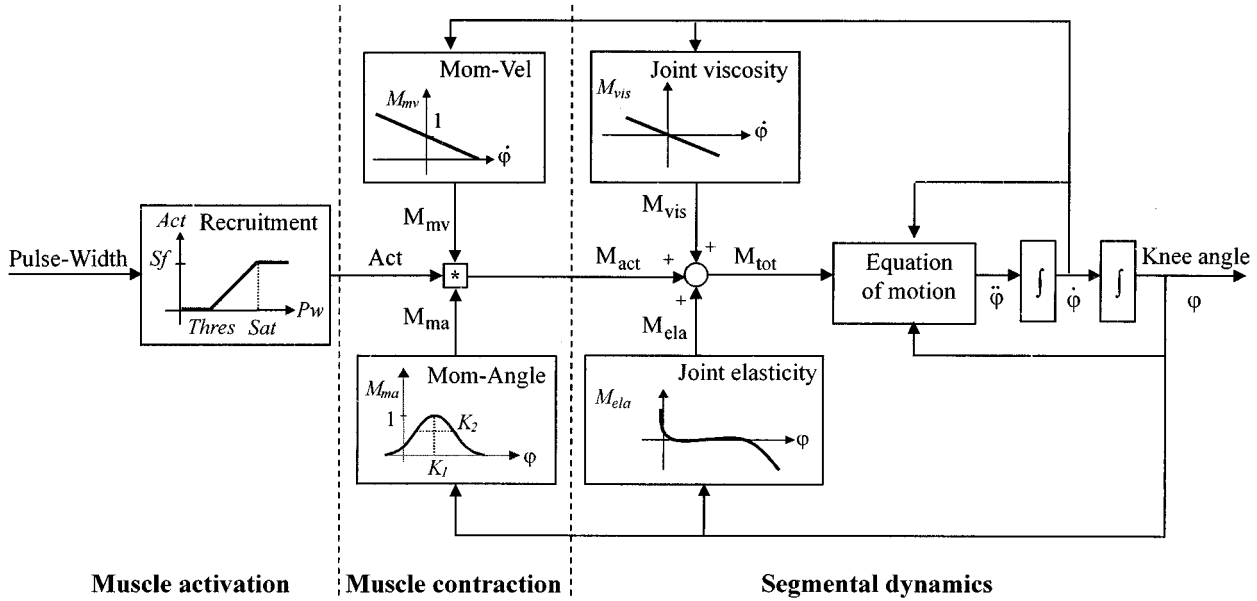
Fig. 1. A schematic representation of the model developed.

human muscles, with the advantages of partially compensating for plant nonlinearity and having a more physiologically oriented interpretation of results. The main disadvantage was the need of an identification phase.

In this study, the role of simulation based on mathematical models was twofold. First, to design, test, and optimize the control strategies, thus reducing time-consuming trial and error adjustments during human experiments. Second, some model components were also implemented in the controller for real-time application (see Section II).

We also focused on the design and evaluation of an adaptive approach. Therefore, a simplified but effective nonlinear dynamic model of the lower limb was developed. It served as a feedforward controller and permitted identification of plant parameters that were considerably time varying. Especially this adaptive control strategy could greatly benefit by the use of mathematical models and computer-based simulations. The convergence and robustness of the adaptation algorithm could, in fact, be safely and efficaciously tested prior to all experimental sessions.

The performances of the different FES control strategies studied in the present paper have been compared in a simplified test bed—the control of knee position of free-swinging leg of seated subjects by means of quadriceps stimulation. This specific experimental condition was often adopted [6]–[8], [12], [14] because it allows the experimenters to perform several experimental sessions (identification procedures, validation tests, analysis of the performance of different controllers, etc.) in a safety and comfortable conditions for the patients. Moreover, the quadriceps muscle plays a fundamental role in the main motor activities (i.e., standing up, sitting down, walking, standing posture, and climbing stairs).

II. METHODS

A. Modeling Approach

If a model is used as a controller, it is necessary to deal with a set of equations that must be solved in real time and a restricted number of parameters that are easy to identify on a specific subject. Therefore, a relatively simple, but nonlinear and physiologically based model, has been designed to be used for real-time controller design. Input to this direct dynamic model is the stimulation pulse width while the output is the knee joint angle. As shown later, this model was then inverted and implemented in the controller. In this model the thigh is positioned horizontally on a bench so that the shank can freely swing about the knee joint. Hip and ankle joints are fixed at a constant angular position. One major restriction of this model is that only the knee extensor muscles can be stimulated. Also, the model is restricted to movements in the sagittal plane and the knee is assumed a hinge joint, in accordance with previous studies which adopted the same experimental setup [6], [14], [15]. In particular Holden *et al.* [16] have shown that the knee joint center location affects slightly the joint dynamics only at normal and fast joint movements.

The model is composed by three parts (Fig. 1): muscle activation, muscle contraction, and segmental dynamics. In the first block the actual muscle activation Act [Nm] is computed from the stimulation pulse width. Stimulation frequency was held constant during all simulations and experiments.

The activation dynamics is modeled using a piecewise linear recruitment function characterized by three values: a threshold pulse width $Thres$ [μs], a saturation pulse width Sat [μs], and a scaling factor Sf [Nm]. Sf is a measure of the muscle strength and the current muscle fitness and is determined by the maximum active moment produced by the muscle at saturation pulse width during isometric contractions at optimum muscle length. Thus, the muscle activation Act can be described in the following way:

$$\begin{cases} Act = 0, & \text{for } Pw \leq Thres \\ Act = \dfrac{Sf}{(Sat - Thres)} \\ \quad \cdot (Pw - Thres), & \text{for } Thres < Pw < Sat \\ Act = Sf, & \text{for } PW \geq Sat. \end{cases}$$

(1)

Other inputs to the muscle contraction block are the knee joint angle and the knee joint velocity used in the moment angle and in the moment-velocity relations. In fact, although muscle force is a function of muscle activation, length, velocity, and maximum isometric muscle force [17], for simplicity, this relation can also be expressed in terms of joint moment and angle [18]. Adapting Hatze's force-length characteristic [19], the moment-angle relation is modeled by a Gaussian function

$$M_{ma} = \exp\left\{ -\left(\frac{\varphi - K_1}{K_2} \right)^2 \right\} \tag{2}$$

where φ is the knee angle ($\varphi = 180°$ is full extension, $\varphi < 180°$ is flexion), and K_1 and K_2 two parameters to be identified. Equation (2) is represented by a typically bell-shaped curve in which the location of the maximum is determined by K_1 and the dispersion around this maximum depends on K_2.

The *moment-angular velocity* relation was derived from a linear approximation of the force-velocity relation f_v as described by Zajac [17]

$$f_v = 1 + \frac{1}{v_m} \frac{dl}{dt} \Rightarrow$$
$$M_{mv} = 1 + \frac{1}{v_m} \frac{dl}{d\varphi} \frac{d\varphi}{dt} = 1 - \frac{1}{v_m} ma_q \dot{\varphi}(t) = 1 - K_3 \dot{\varphi}(t) \tag{3}$$

where l is the quadriceps muscle length, v_m is the maximum contraction velocity, and $ma_q = -dl/d\varphi$ is the knee-moment arm of the quadriceps muscle (the negative sign is due to the knee angle convention: during a concentric movement, l decreases and φ increases). Maximum contraction velocity can be approximated from the percentage of slow muscle fibers and the optimum muscle length as described by Winters *et al.* in [20] and [21]. Muscle and joint specific parameters (v_m and ma_q) are then summarized in the constant $K_3 = ma_q/v_m$. The output of the muscle contraction block is the active muscle moment computed by

$$M_{\text{act}} = Act \cdot M_{ma} \cdot M_{mv}. \tag{4}$$

While M_{ma} and M_{mv} are unit-less variables, Act and M_{act} are expressed in [Nm].

In this model, a separation was made between the active and the passive muscle properties. So far only the former have been considered. All passive muscle characteristics (viscosity and elasticity) are assigned to the knee joint and are included in the second part—the segmental dynamic block.

The motion can be described by

$$M_{\text{tot}} = \frac{d\Gamma(t)}{dt} = J_k \cdot \ddot{\varphi}(t) \tag{5}$$

where J_k is the moment of inertia and $\Gamma(t)$ is the momentum of the shank-foot complex referred to the knee joint.

The total external moment acting on the knee joint in (5) is computed by summing active, gravitational, and passive moments

$$M_{\text{tot}} = M_{\text{elastic}} + M_{\text{viscous}} + M_{\text{grav}} + M_{\text{act}}. \tag{6}$$

The passive viscous moment is modeled by a linear knee damping function [15] while knee elasticity is modeled by a double exponential function as proposed in [22], [23].

The center of gravity (COG), together with the mass m of the shank and the moment of inertia about the COG J_{COG}—all three parameters being specific-patient constant properties—were identified using the Zatsiorsky regression equations [24]. Although these equations were identified on healthy subjects, their application on shank and foot segments of paraplegics should not produce significant errors. In fact, the influence of mass reduction (related to possible muscle atrophy of SCI patients) on the inertial property of the shank-foot complex is very low since lower leg muscles are either quite small or mainly concentrated on the proximal part of the shank (calf muscles).

In order to simulate the lower limb of a paraplegic subject, we adopted a more complex model previously developed by Riener *et al.* [25]. We call this model "plant simulator." In the plant simulator five muscle groups spanning the human knee joint are considered: biarticular (*biceps femoris* long head, *semitendinosus*, *semimembranosus*), and monoarticular (*biceps femoris* short head) knee flexor muscles, biarticular and monoarticular knee extensor muscles (*rectus femoris* and *vasti muscles*, respectively) and biarticular ankle plantarflexors (lateral and medial *gastrocnemius*).

Inputs to the plant simulator are the modulated pulse widths and pulse frequencies produced by the stimulator and delivered to each muscle through surface electrodes. The plant simulator output is the computed knee joint position as resulting from stimulating different muscle groups or also from passive oscillations. The muscle groups can be treated independently and they differ in activation parameters (contraction time, recruitment threshold, etc.) as well as contraction parameters (muscle length, isometric force, etc.). If only the quadriceps muscle is stimulated the other muscles still contribute to the limb dynamics by their passive viscous and elastic properties. Other properties of the plant simulator that are different from the simplified model are as follows: for the plant simulator the recruitment curve is described by a nonlinear function instead of a piecewise linear function. Also, different groups of motor units are considered. To calculate the muscle activation and deactivation dynamics an additional second-order function describing the calcium dynamics of the muscle is added. The muscle contraction dynamics are not modeled in the angle/moment, but rather in the muscle length–force space. The muscle paths and the geometry of the knee joint with changing lever arm are modeled in more detail instead of assuming a simple hinge joint.

The number of simplifications introduced in the simplified model compared to the plant simulator allowed the invertibility of the model, made feasible the real-time resolution of model equations and reduced the complexity of the parameter identification experiments.

B. Control Strategies

1) Open-Loop Control: The inversion of the developed direct model made it possible to estimate the pulse width required to perform a desired knee angle trajectory. In a first step, after double differentiation of the desired knee joint trajectory, the
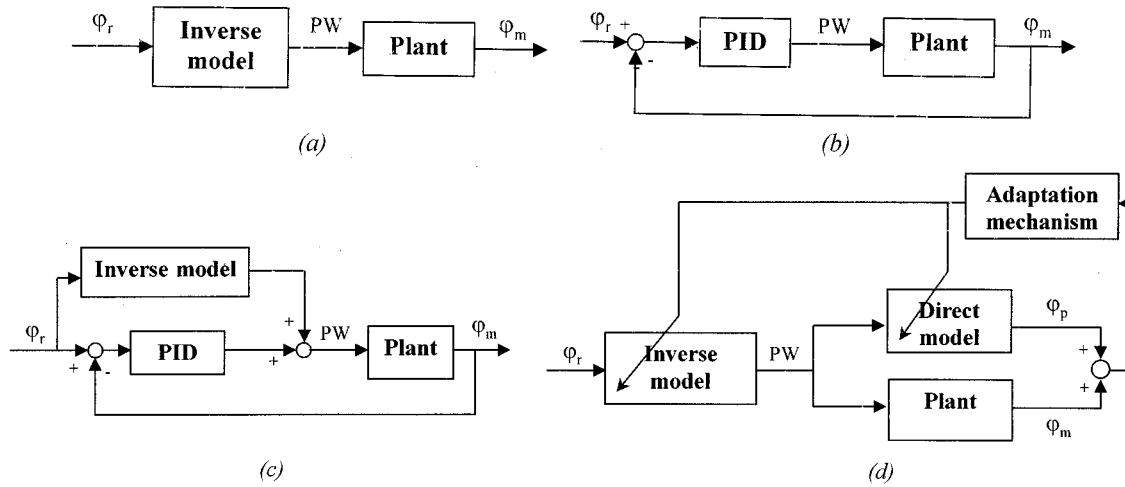
Fig. 2.   Block diagrams of the control strategies implemented. (a) The open-loop control. (b) The feedback PID control. (c) The combination of feedforward and feedback control. (d) The adaptative approach. In (d) the adaptation mechanism is driven by the error (ε) between the angle predicted by the direct model (φ_p) and the measured knee angle (φ_m). φ_r is the reference knee angle and PW the pulse width stimulation.

total moment M_{tot} is computed by (5). An estimate of the required active moment M_{act} is then obtained by subtracting the passive moments and the gravitational moment M_{grav} from the M_{tot}. In a second step, the inverse muscle contraction is modeled. The required active moment previously computed is multiplied by the inverse moment angle and inverse moment velocity relations. This results in the following activation function:

$$ Act = M_{\mathrm{act}} \cdot \exp\left\{ \left(\frac{\varphi - K_1}{K_2} \right)^2 \right\} \cdot (1 - K_3 \cdot \dot{\varphi}(t))^{-1}. \quad (7) $$

In the last step, by using the inverse recruitment curve, the required pulse width is calculated.

The entire inverse dynamic model was used as a nonlinear compensation block in series with the plant simulator in order to cancel out part of the nonlinearities of the system [Fig. 2(a)]. Due to model approximations and system components impossible to invert (e.g., time delays, saturation effects), the cancellation of all nonlinearities was not exact. The goal of this control approach is therefore to get as close as possible to an overall zero-order linear system.

2) Feedback Control: A PID controller was used [Fig. 2(b)]. The PID controller parameters were firstly identified in the simulations using an iterative procedure based on the minimization of root mean square (rms) error [7], where the initial guess of the optimization was derived by Ziegler–Nichols rules [5]. Then, a further adjustment to the single patient was performed with a trial and error procedure at the beginning of the experimental session.

3) Combination of Feedforward and Feedback Control: The third controller we considered, resulted from a combination of the previous two approaches [7], [8], where the feedback controller is intended to compensate for model errors and/or any external or internal disturbances.

The total pulse width (*PW*) delivered to the plant was the sum of the pulse width predicted by the inverse model in the feedforward loop and the pulse width resulting from the PID controller [Fig. 2(c)].

It was excluded to simply insert the inverse model between the PID controller and the plant because of the high sensitivity of the inverse model to sensor noise that would have introduced large errors in the PW if the output of the PID controller were used as input to the model.

4) Adaptive Control: In the adaptive control strategy [Fig. 2(d)] the inverse dynamic model delivers the predicted pulse width both to the plant and the direct dynamic model. The direct and the inverse dynamic models are identical except that they are "reversed" with respect to each other. In this approach, the direct dynamic model is an "observer" of the plant. The error between the knee angle predicted by the direct dynamic model and the one resulting from the plant drives the adaptation mechanism. This mean error (averaged over a moving window) is minimized by changing two time-varying parameters of the model. The same changes are then fed into the inverse dynamic model in order to optimize the feedforward controller. Due to their considerable time shifting, the two parameters chosen for the adaptation were the scaling factor Sf—a measure of the muscle strength and fitness which is proportional to the maximum active moment—and the pulse width threshold $Thres$. The following relations describe the iterative laws that permitted on-line adaptation:

$$ Thres_t = Thres_{t-1} + G_1 \cdot \overline{\varepsilon}_t \quad (8) $$

$$ Sf_t = Sf_{t-1} + Sf_{t-1} \cdot G_2 \cdot (1 - GR) + G_3 \cdot \overline{\varepsilon}_t \quad (9) $$

where $\overline{\varepsilon}_t$ is the mean error between the predicted and the measured knee angles, G_i ($i = 1, 2, 3$) are the fixed adaptation gains, and GR is the ratio between the standard deviation of the predicted knee joint trajectory (φ_p) and the standard deviation (STD) of the measured trajectory (φ_m).

$$ GR = \frac{\mathrm{STD}(\varphi_p(t))}{\mathrm{STD}(\varphi_m(t))}. \quad (10) $$

The standard deviation of the joint angle is a measure for the effective amplitude of the movement, which proved to be more

Subject	Sex	Age [yrs]	Time after injury [yrs]	Level of SCI	FES training [yrs]
MM	Female	40	15	T7	4
BH	Male	33	3	T1	2

reliable than the peak-to-peak amplitude in computer simulations. The algorithm can be applied for movements that are periodic. Thus, the moving window length is an entire multiple of the reference trajectory period. The implementation of the moving window allowed that the period length changes over time (wobbling).

When, for example, the averaged error is positive ($\overline{\varepsilon}_t > 0$) it means that being the knee less extended than desired, a higher pulsewidth is required from the inverse dynamic model. This is achieved by rising the threshold and, simultaneously, decreasing the scaling factor in order to produce a shift of the recruitment curve toward higher pulse width values, without affecting the slope (of course this implies also a reduction of the maximum active moment). The changing rate of $Thres$ and Sf, as a function of $\overline{\varepsilon}_t$, depends on G_1 (a positive number) and on G_3 (negative), respectively.

Basically, a shift of the recruitment curve minimizes offset errors between the measured and predicted knee angles. On the other hand, changes in the slope mainly affect the amplitude of the measured angle trajectory and, therefore, are used to minimize errors due to different displacement around the mean values. In fact, the parameter $Thres$ settles down at a constant value as soon as the measured and predicted angles have the same mean value within the moving window; while Sf stabilizes when those angles have also the same STD. The positive constant G_2 weights the effects of different STD between measured and predicted angles. The values of constants G_i have been tuned through simulations using a trial and error procedure, according to their role in the adaptation algorithm. Moreover, care was taken that, as it can be easily demonstrated, in order to maintain a constant slope of the recruitment curve when only offset errors are present, the ratio between G_1 and G_3 must be in the order of $(Sat - Thres)/Sf$. A good compromise between adaptive algorithm convergence and system stability was found for $G_1 = 2.0$ μs/deg, $G_2 = 0.004$, and $G_3 = -0.1$ N/deg. In general, it was found that for higher absolute values of the gains, the response of the adaptive controller was faster but with a tendency to system instability.

C. Experimental Approach

The control strategies were tested on two subjects with complete thoracic spinal cord injury (Table I). Both of them had undergone a preliminary muscular conditioning program. Inclusion criteria included: absence of significant contracture and full range of motion at the knee joint. The quadriceps muscles did not exhibit significant active spasms during the experiments, which were performed without any antispastic pharmacological treatment. Each subject voluntarily participated at two ex-

perimental sessions. The first one served to identify the musculo-skeletal parameters (identification session), while during the second, the control strategies were applied (control session).

The subjects sat on a bench, which allowed the lower leg to swing freely, while the hip angle was fixed at 60° of flexion (see Fig. 3). The quadriceps muscle was stimulated using adhesive surface rectangular electrodes (5×9 cm^2 Pals electrodes, Axelgaard Manufacturing Co., Fallbrook, CA) with the cathode placed just proximally over the estimated motor point of rectus femoris and the anode approximately 4-cm proximal of the patella. In this way, it is reasonable that also the other heads of the quadriceps have been activated. However, since in our study the hip joint was maintained in a fixed position, the distinction between mono- and biarticular knee extensor muscles has no functional effect. A computer driven stimulator delivered balanced bipolar rectangular pulses. Pulse width modulation (from 0 to 520 μs) with constant current amplitude (80 mA for subject MM and 100 mA for subject BH, depending on their muscular response) and 20-Hz stimulation frequency was used.

The knee joint angle was monitored by an electrogoniometer, which included two potentiometers connected by a telescopic arm. One potentiometer was fixed at the thigh and the other one at the shank. The measured signals were sampled at 160 Hz by a 12-bit analog-to-digital converter and stored in the personal computer for offline analysis. A low-pass filtering and a resampling at 20 Hz was then performed.

Reference trajectories were wobbling sinusoidal waves (min–max: 105–155° for MM and 105–165° for BH) at changing frequencies (from 0.13 Hz to 0.4 Hz in 40 s), in order to monitor different working frequency ranges. A series of at least five tracking tests was performed with each controller. Additionally, several trials were performed at the beginning of each series, to optimally adjust the controller parameters to a specific subject. Intertrial resting intervals of at least 10 min were used to reduce the effects of fatigue. The duration of the identification session and of the control session was about 2 and 3.5 h, respectively.

D. Performance Indexes

Two indexes have been used to assess and compare the controllers' performances: a time-lag error TL and a tracking error Tr between the reference trajectory φ_r and the actual joint angle φ_m pattern. These two indexes allowed us to discriminate between the tracking performance and the delay introduced by the controller. The time-lag was evaluated using the cross-correlation function between the reference and the obtained trajectory. In particular, the time delay τ at which the correlation had a maximum was considered as the TL error; that is

$$TL = \tau \qquad \text{for } \max \Re_{\varphi_r \varphi_m} = \max \left(\sum_{t=1}^{N} \varphi_r(t)\varphi_m(t+\tau) \right).$$

$$(11)$$

Once the TL error has been quantified and compensated by shifting the actual angle trajectory, the Tr error was computed
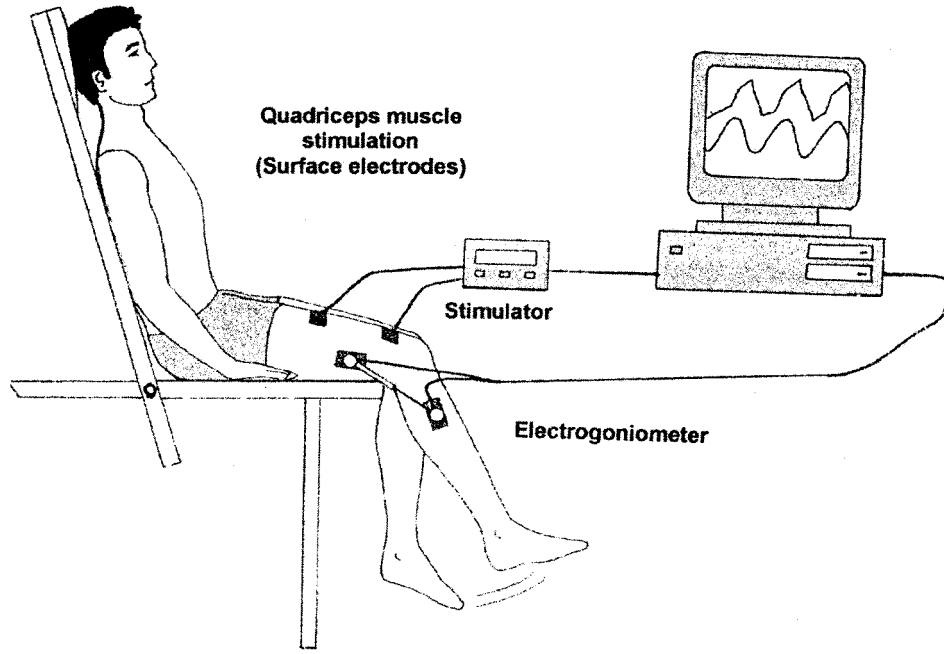
Fig. 3. Illustration of the experimental setup.

as the rms error between the reference and the actual knee angles

$$Tr = \sqrt{\left(\frac{\sum_{t=1}^{N}(\varphi_r(t) - \varphi_m(t+TL))^2}{N}\right)} \qquad (12)$$

where $N = n°$ of samples of a given period.

Since the reference trajectories were wobbling sinusoids, the computation of both the TL and Tr errors was performed at each period to verify that they were independent of the frequency. These indexes allowed to quantitatively assessing that a decrease of the errors versus time was achieved with the adaptation algorithm.

E. Model Identification

In order to identify patient-specific parameters for both the inverse model and the plant simulator, the following set of experiments was performed: stimulation experiments under isometric conditions; passive pendulum tests; and quasistatic passive movements of the knee.

Under isometric conditions the shank was attached to an adjustable support. This was equipped with a strain-gauge-based force transducer to measure the knee joint moment produced by the stimulated quadriceps muscle. A series of measurements with the knee joint fixed at different angular positions, ranging from $90°$ to $160°$ of knee extension, were accomplished. These isometric information permitted an off-line identification of the parameters within the muscle activation and contraction blocks ($Thres$, Sat, Sf, K_1, and K_2). The parameter K_3 was not individually identified since it was difficult to determine, therefore

it was computed from data available in literature as described in [2], [18].

To identify the segmental dynamics block two different approaches were applied. Knee joint viscosity was evaluated by passive pendulum tests [26], while passive elastic parameters were obtained from measurements with quasistatic movements of the shank [22], [23].

To measure the passive elastic knee joint moments as a function of joint angle, the experimenter slowly moved the distal limb (≈ 2–5 deg/s) in the sagittal plane by pulling or pushing a handle attached to a strain-gauge force transducer. Identified parameters for both subjects are presented in Table II.

III. RESULTS

A. Model Validation

For model validation, the quadriceps muscle was stimulated with triangular pulse width modulation patterns (0–500 μs) with the shank freely swinging. A comparison between experimental and simulation results is shown in Fig. 4. The performance of the identified model was quantitatively assessed by computing the rms error between the predicted φ_p and the measured knee joint angle φ_m. For subject MM the rms error was about $9.8°$, which corresponded to 14% of the angle range covered. For patient BH the rms error was $13.2°$, corresponding to 17% of the knee angle range.

An interesting observation is that for both subjects the measured knee joint trajectory presented an asymmetric behavior between the ramp up and the ramp down phase, meaning a difference between concentric and eccentric contractions not adequately considered in the model [in the model only the moment-angular velocity relation is dependent on the direction of the movement [see (3)].
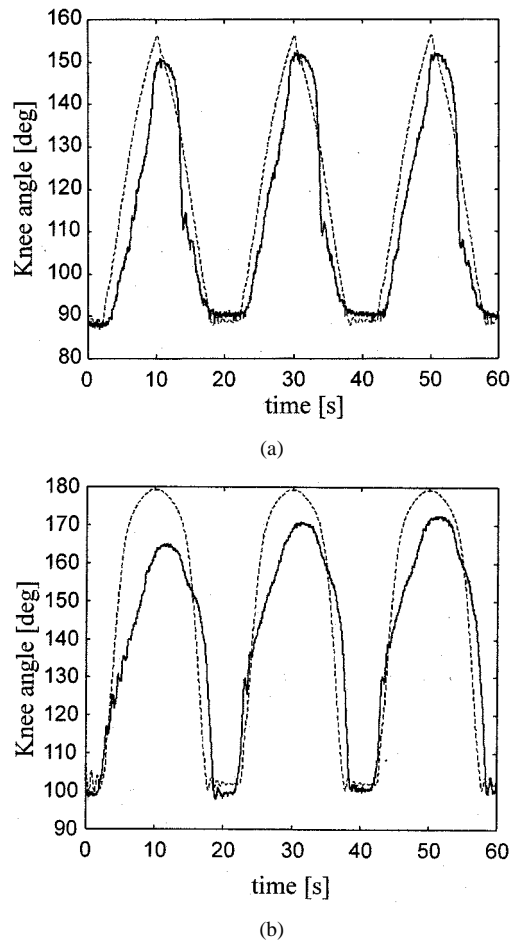
(a)

(b)

Fig. 4. Model validation. Comparison between measured (solid line) and simulated (dashed line) knee angle trajectory during open-loop stimulation with a triangular modulation of PW (from 0 to 500 μs in 10 s). (a) Subject MM. (b) Subject BH.

The same validation procedure was carried out for the plant simulator identified on patient MM. The rms error was 8.3°, which corresponds to 11% of the angle range. However, the little difference between the two rms values found for the two different models justifies the use of the developed simplified model in the controller.

B. Simulation Results

All simulations were done with the plant simulator adjusted to subject MM. Fig. 5 shows some examples of simulation results obtained with the open-loop control, the feedback control and their combination. In the open-loop configuration, the error between the desired and the simulated angles was significant [Fig. 5(a)]. The main differences between angle trajectories consisted in the larger range for the simulated angle compared to the desired angle and in a non linear rise and decrease of simulated angular values. The PID controller reduced the tracking error, whereas some oscillations have been introduced. With the combination of feedforward and feedback control, both tracking error and oscillations were reduced.

As for the adaptive controller, simulation was used to evaluate the convergence and robustness of the algorithm before its experimental application on the patients. The convergence was tested by setting erroneous initial values of the threshold pulse
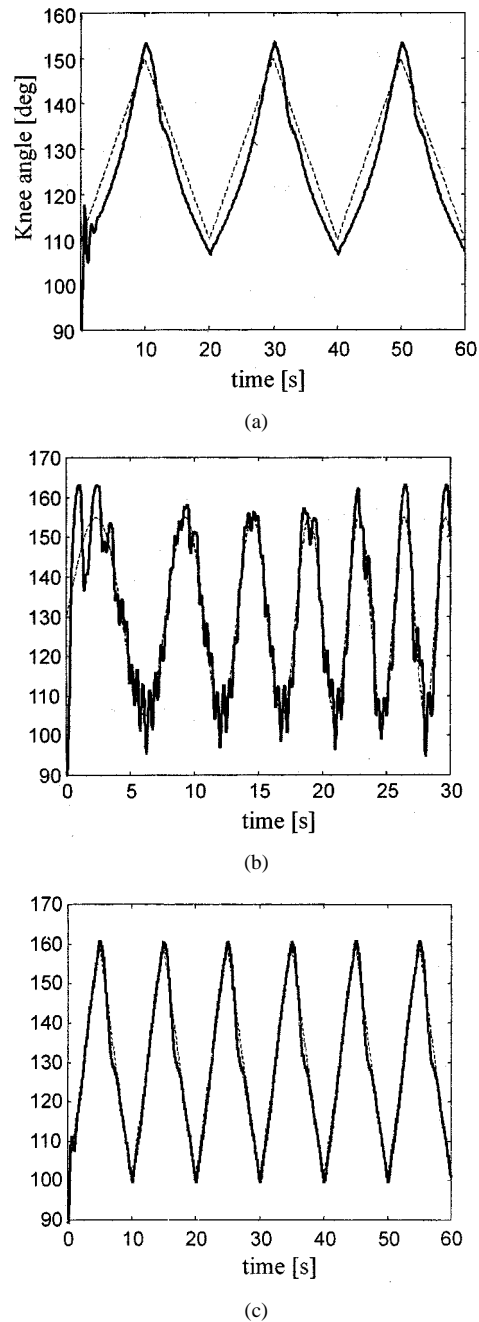

(a)

(b)

(c)

Fig. 5. Simulation results obtained from nonadaptive control approaches. (a) Open-loop control. (b) Feedback PID control. (c) Feedforward plus feedback control. The dashed line is the reference knee angle trajectory (φ_r), while the solid line is the obtained angle (φ_m). 180° is full knee extension.

width and of the scaling factor (see Fig. 6). To evaluate the robustness of the algorithm qualitatively, some internal changes and external disturbances were triggered, as typically performed in control system theory (e.g., [32]). In particular, a step-up of $Thres$ and of the leg mass was simulated (see Fig. 7).

C. Experimental Results

Examples of actual knee joint trajectories obtained with the three fixed controllers are shown in Fig. 8, where the considered reference trajectory is reported too. All the experimental trials quantitatively confirmed the qualitative results obtained in simulations. The performances of each controller in both patients

TABLE II
PATIENT-SPECIFIC PARAMETERS

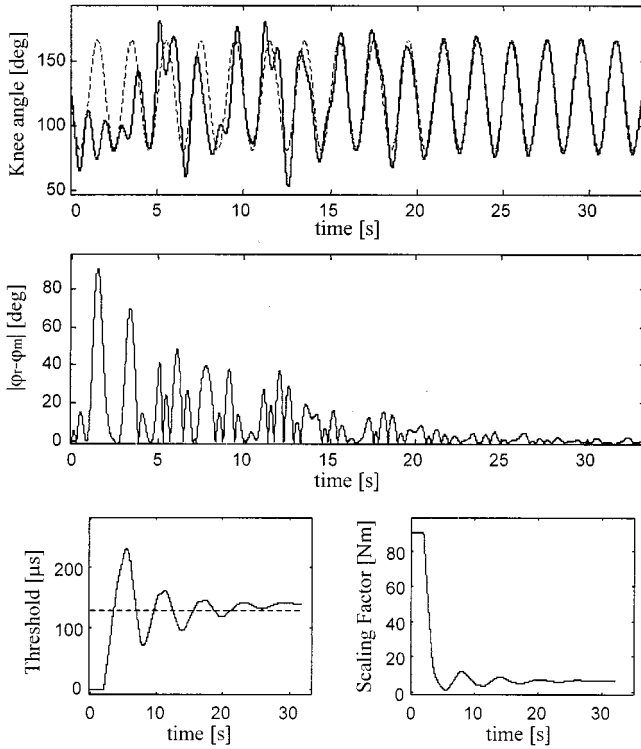| Subject	Sf [N·m]	$Thres$ [μs]	Sat [μs]	K_1 [deg]	K_2 [deg]	K_3 [rad⁻¹·s]	K_{damp} [rad⁻¹·s]	COG [m]	M [kg]	J_{cog} [N·m²]
MM	10.5	130	500	60	65	0.04	0.11	$19·10^{-2}$	2.7	$25·10^{-2}$
BH	15	100	500	50	65	0.04	0.11	$25·10^{-2}$	3.5	$35·10^{-2}$

Fig. 6. The convergence of the adaptive algorithm tested in simulation. (a) Reference φ_r (dashed line) and obtained φ_m (solid line) knee angle plotted versus time. (b) Norm of the error between reference and obtained knee angle. (c) Threshold and scaling factor versus time. The dashed line is the goal threshold (130 μs). The initial wrong values were $Thres = 0$ μs and $Sf = 90$ Nm.
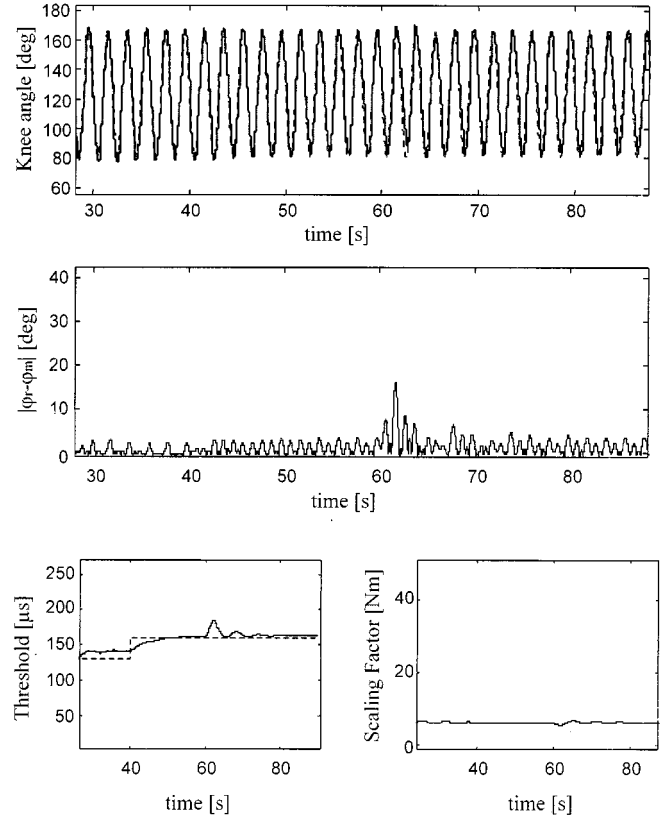

Fig. 7. The robustness of the adaptive algorithm tested in simulation. At $t = 40$ s the threshold was suddenly changed from 130 μs to 160 μs, while at $t = 60$ s the mass of the leg was increased to three times its original value, from 2.7 Kg to 8.1 Kg. (a) Reference φ_r (dashed line) and obtained φ_m (solid line) knee angle. (b) Norm of the error between reference and obtained knee angle. (c) Threshold and scaling factor versus time. The dashed line is the goal threshold.

are compared in Table III, where the TL and Tr errors (mean and SD of all trials) are reported. In both patients the PID controller reduced the Tr error but increased the TL error, while the combination of feedforward and feedback control reduced both Tr and TL errors.

With regards to the adaptive control, the initial guesses of the two parameters to be adjusted, i.e., $Thres$ and Sf, were set to the same erroneous values used in the simulations in order to test the algorithm convergence in presence of sensor noise and parameter uncertainty. The resulting knee angle traces and the parameter adaptations are shown in Fig. 9 for both subjects.

The cycle by cycle error analysis showed that both TL and Tr errors decreased versus time (Fig. 10) assuming values similar or lower to those shown by not adaptive controllers (Table III).

IV. DISCUSSION

Different approaches can be adopted to compensate for the nonlinear behavior of the plant, like "black box" modeling [14], artificial neural networks [8], [28]–[31] fuzzy logic control [32], [33] and physiologically based inverse dynamic modeling. The latter approach, adopted in the present study, has the advantages to allow for a separate identification of the different parameters of the model, to allow the calculation of different intermediate variables (e.g., joint moments or activation functions) and, in general, to get a better understanding about the significance of the different physiological processes. The drawbacks are mainly related to the complexity and accuracy of parameter identification.

In our study a different behavior in concentric and eccentric contractions was found between real and simulated knee trajectory. This was confirmed also in the experiments with the open-loop strategy, where a different agreement between reference and actual trajectories was found during concentric contractions compared to eccentrics contraction of the quadriceps, corresponding to knee extension and flexion phases, respectively. One explanation is that stretch reflexes, which were
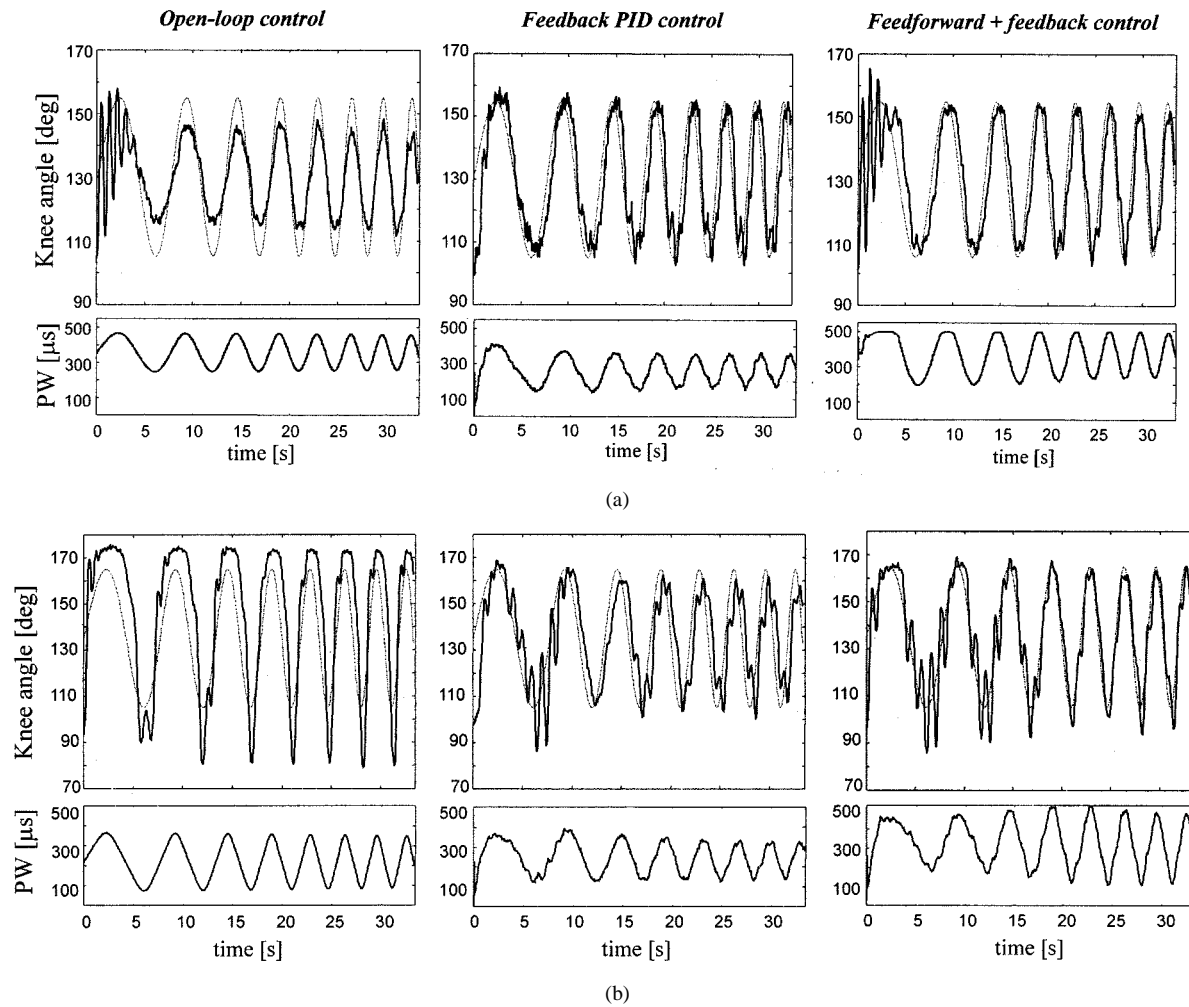
Fig. 8. Experimental results obtained with nonadaptive control approaches for (a) subject MM and (b) subject BH. The first column is related to open-loop control, the second column to feedback PID control and the third column to the combination of feedforward and feedback control. Dashed line is the reference knee angle (φ_r) and solid line is the measured knee angle (φ_m) trajectory. Below each graph, the time course of the correspondent pulse width is shown.

TABLE III
SUMMARY OF CONTROLLERS PERFORMANCE INDICES (MEAN ±SD; $n = 5$). A = OPEN-LOOP CONTROL; B = FEEDBACK CONTROL; C = COMBINATION OF A AND B

Subject	Controller	Time-lag error [s]	RMS error [deg]
MM	A	0.13 ± 0.05	8.2 ± 2.3
MM	B	0.24 ± 0.08	4.6 ± 0.7
MM	C	0.21 ± 0.02	3.4 ± 0.3
BH	A	0.23 ± 0.12	15.1 ± 1.9
BH	B	0.33 ± 0.08	7.3 ± 2.4
BH	C	0.15 ± 0.09	5.7 ± 2.6

not considered in the model, occur during muscle lengthening and generate this asymmetric behavior in the shank movements. A temporal asymmetry between cross bridge formation and breaking may also play a role. An advanced model comprehending also those aspects is under testing [34].

The effects of the simplifications introduced in the developed model compared to the more complex plant simulator are clearly shown in the simulations with the open-loop controller. The incomplete compensation of plant nonlinearity showed by Fig. 5(a) can be explained by the use of muscle activation and contraction blocks at a joint level (in terms of joint moment and angle), in the inverse model, instead of a description for each muscle (in terms of muscular force and length). Therefore, the global parameters of the inverse dynamic model $Thres$, Sat, Sf, K_1 and K_2 are only an approximation of the correspondent parameters at muscular level used in the plant.

It was found that the performance of the open-loop control strategy is highly affected by the accuracy of the identification procedure and by the presence of time-varying parameters in the process. In subject BH, for example, the real recruitment curve might have a steeper slope than the one identified and used in the inverse model. This inaccuracy might explain the increased range of the measured knee trajectory compared to the reference trajectory [see Fig. 8(b), open-loop control].

In patient MM is visible the opposite effect [Fig. 8(a), open-loop control]: an overestimation of the maximum active moment, which limited the range of the PW of the stimulation delivered to the subject and, as a consequence, reduced the range of the knee angle trajectory. Another critical aspect of feedforward open-loop control is that it can not compensate for any unknown
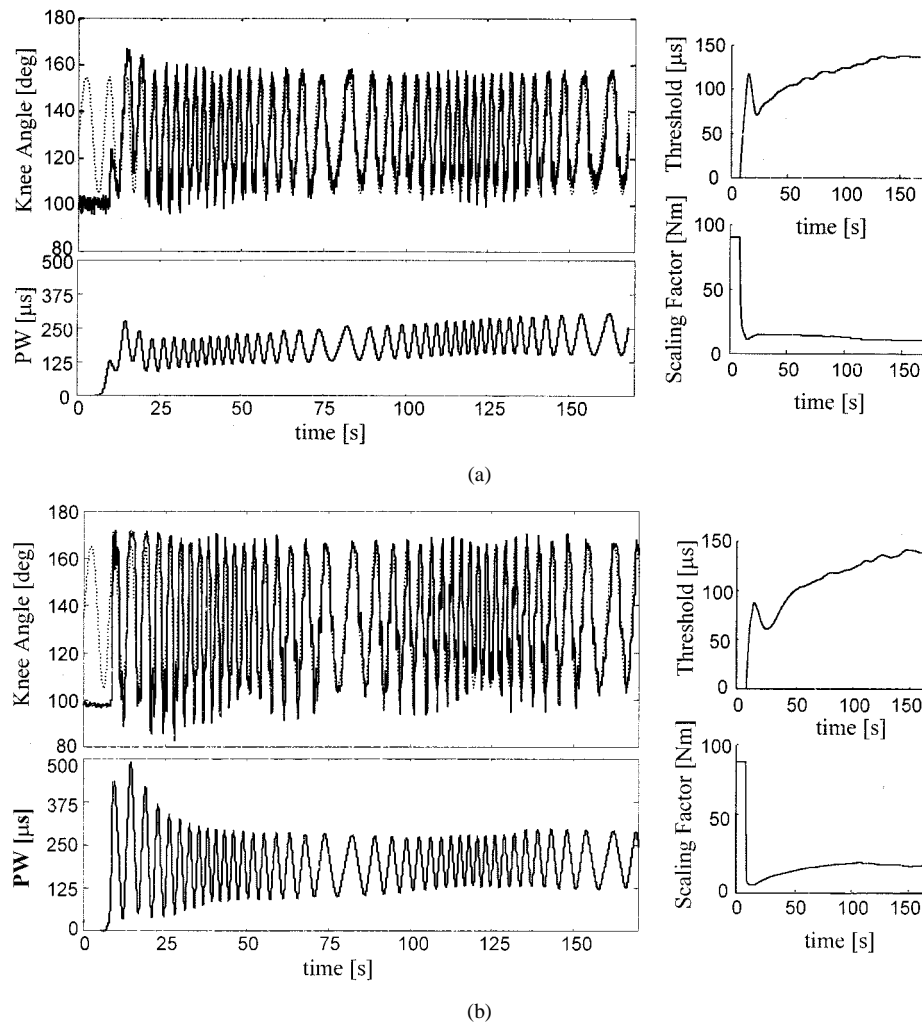
Fig. 9.   Adaptive approach. Experimental results for subject (a) MM and (b) BH. On the right, reference φ_r (dashed line) and measured φ_m (solid line) knee angles. On the left, parameters adaptation during the same trials. Due to its nature, the adaptive algorithm and, therefore, the modulation of parameters and the delivery of stimulation started after one complete period, i.e., 10 s in this example.

external disturbance, that is likely to occur during functional applications of FES. Although a linear PID controller could not take into account the nonlinearity of the plant, an improvement in the tracking error was achieved for both patients with this controller. However, time-lag errors increased more than double compared to the open-loop configuration, due to the inherent delay of the feedback. It is interesting to observe that the time-lag between reference and actual trajectory was constant in time and, thus, frequency-independent, although the reference trajectory had a variable frequency [see Fig. 8(a) and (b), feedback PID control]. Both on simulations and experiments the combination of feedforward and feedback strategies improved the quality of the control: the Tr errors became substantially smaller and the TL errors went down to values similar to those of the open-loop strategy (Table III). This was possible because the nonlinear compensation provided by the feedforward inverse model is combined with the capability of the PID feedback controller to reduce steady-state errors [see Figs. 5(c), 8(a) and (b), feedforward + feedback control]. These results are in accordance with the work of Chang *et al.* [8] where the feedforward component was based on a neural network. Although, in that study no specific indexes were computed to quantify the different delays

due to each controller configuration, from the graphs presented in their paper [8], the decrease of time lags due to the inverse feedforward component is apparent.

Concerning the adaptive control, the simulations showed that the parameters' convergence to their real value was reached in about 20 s (Fig. 6) and that the controller was able to compensate for the artificially generated large disturbances in few seconds (Fig. 7). Similar parameter convergence, however a little bit slower, was obtained during the experiments on patients. Interestingly, in both patients, the pulse width threshold continued to increase slowly within the experiments (see Fig. 9), indicating a moderate increase of muscle fatigue. This underlines the limitation of control strategies based on models with fixed parameters.

It is emphasized that the adaptive approach could be used also to identify subject-dependent parameters that present high time-dependency or that cannot be measured directly, although additional work must be done to theoretically evaluate the dependence of algorithm convergence on gains. A further limitation of the on-line identification capability of the adaptive approach, is related to the possible presence of internal or external disturbances (e.g., obstacles, spasms). For these reason, an automatic detector of irregularly appearing disturbances that ex-
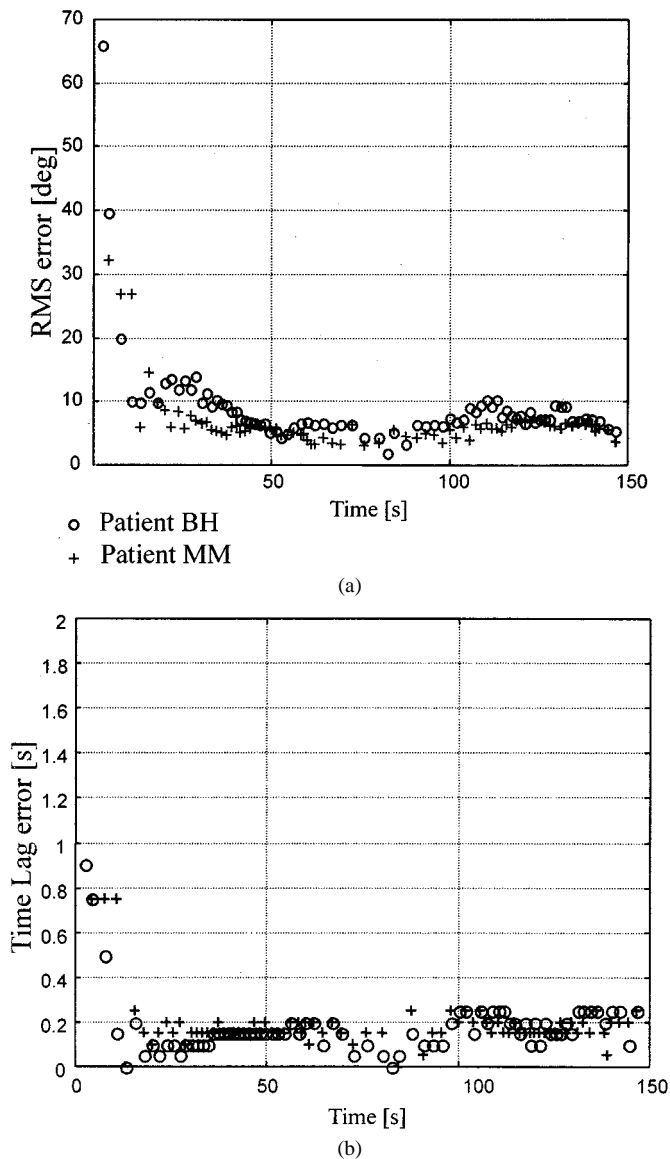
Fig. 10. Adaptive controller. Experimental results. (a) Time course of time lag error (TL). (b) Time course of rms errors (Tr). Note that the TL error is always a multiple of the sampling period (0.05 s).

cludes the adaptation mechanism during the period of time when these disturbances occur, should be introduced.

Compared to the considered controllers based on a PID (b and c control strategies), the adaptive controller here presented is less demanding with respect to the quality of sensor signals since the measured signal is not used directly to define the PW.

A question could be raised about the use of an observer rather than using directly the differences between the reference and the measured trajectory as the input to the adaptive controller. In fact, one could say that since one system (the inverse model) is in series to its own inverse (the direct model or observer), the predicted output of the observer (φ_p) should be identical to the reference trajectory (φ_r). First of all, this might not be true if saturation occurs, i.e., if the pulse width required for a given reference angle trajectory is above the saturation level. Second, this architecture allows the combination with an additional closed-loop controller (e.g., a PID controller, whose output is added to the output of the inverse model) without any

modification of the adaptive controller. In this way, the advantages of the feedforward plus feedback controller approach are combined with the parameters on-line adjusting capability of the adaptive controller. If the presence of two simultaneously operating feedback controllers showed to be problematic, a possible solution would be to implement a switch that excludes the PID controller and activates the adaptive algorithm when needed (e.g., fatigue onset).

V. CONCLUSION

The problem of an effective and reliable control of stimulation parameters is the main aspect examined in this work. In particular it has been shown how the relevant nonlinearity of the system can be partially compensated through an appropriate modeling approach and how the tradeoff between complicated models and the possibilities of parameter identification can justify some simplifications.

Although the limited number of subjects considered in the present work does not allow generalizing our findings, by considering the four control strategies here presented and the results of simulations and experimental tests, the following achievements can be summarized.

Inverse dynamic models can compensate for most of the nonlinearity of the system assuming that the model has been identified properly. Computer simulations and on-line adaptive algorithm support the identification procedure.

Closed-loop controllers (here the PID), yield better tracking control but considerable increase in time lag. The latter can be reduced by adding a feedforward inverse dynamic model.

The efficacy of the inverse dynamic model as a compensator of system nonlinearity can be considerably improved by using an adaptive approach that accounts for time-variant effects.

The adaptive controller proposed in this study permitted a continuous on-line compensation of two critical model parameters and showed robustness and reasonable adaptation speed. Although it has been developed and tested in a simplified situation, i.e., the control of a single joint movement, the present adaptive algorithm is applicable for generic periodic movements such as walking or ascending and descending stairs. Of course, a more complex model is required when multiple joint movements are considered. Moreover, specific procedures to define the reference trajectory for a given motor task must be developed, for example using optimization algorithms to minimize joint moments during standing up [35] or optimizing the trajectory of swinging limb during walking [36].

It can be expected that lower extremity FES systems will become more reliable and widespread aids for persons with paraplegia, provided that efficient and robust control systems will be made available. We believe that model-based approaches and the application of computer simulations will play an important role to achieve this goal.

REFERENCES

[1] J. M. Hausdorff and W. K. Durfee, "Open-loop position control of the knee joint using electrical stimulation of the quadriceps and hamstrings," *Med. Biol. Eng. Comput.*, vol. 29, pp. 269–280, 1991.

[2] J. Quintern, R. Riener, S. Volz, S. Rupprecht, and A. Straube, "Inverse model for control movement," in *Neuroprosthetics from Basic Research to Clinical Applications*, A. Pedotti, M. Ferrarin, R. Riener, and J. Quintern, Eds. Berlin, Germany: Springer-Verlag, 1996, pp. 255–262.

[3] R. J. Jaeger, "Design and simulation of closed-loop electrical stimulation orthoses for restoration of quiet standing in paraplegia," *J. Biomech.*, vol. 19, pp. 825–835, 1986.

[4] A. J. Mulder, P. H. Veltink, and H. B. K. Boom, "On/off control in FES-induced standing up: A model study and experiments," *Med. Biol. Eng. Comput.*, vol. 30, pp. 205–212, 1982.

[5] M. Ferrarin, E. D'Acquisto, A. Mingrino, and A. Pedotti, "An experimental PID controller for knee movement restoration with closed loop FES system," in *Proc. 18th Annu. Int. Conf. IEEE—EMBS*, Amsterdam, The Netherland, 1996, 386.

[6] P. H. Veltink, "Control of FES-induced cyclical movements of the lower leg," *Med. Biol. Eng. Comput.*, vol. 29, pp. NS8–NS12, 1991.

[7] J. Quintern, R. Riener, and S. Rupprecht, "Comparison of simulation and experiments of different closed-loop strategies for functional electrical stimulation: Experiments in paraplegics," *Artificial Organs*, vol. 21, pp. 232–235, 1997.

[8] G.-C. Chang, J.-J. Luh, G.-D. Liao, J.-S. Lai, C.-K. Cheng, B.-L. Kuo, and T.-S. Kuo, "A neuro-control system for the knee joint position control with quadriceps stimulation," *IEEE Trans. Rehab. Eng.*, vol. 5, pp. 2–11, Mar. 1997.

[9] R. Riener, J. Quintern, and G. Schmidt, "Biomechanical model of the human knee evaluated by neuromuscular stimulation," *J. Biomech.*, vol. 29, no. 9, pp. 1157–1167, 1996.

[10] L. A. Bernotas, P. E. Crago, and H. J. Chizeck, "Adaptive control of electrically stimulated muscle," *IEEE Trans. Biomed. Eng.*, vol. BE-34, pp. 140–147, 1987.

[11] M. S. Hatwell, B. J. Oderkerk, C. A. Sacher, and G. F. Inbar, "The development of a model reference adaptive controller to control the knee joint of paraplegics," *IEEE Trans. Automat. Contr.*, vol. 36, pp. 683–691, June 1991.

[12] J. Reis and J. J. Abbas, "Adaptive neural network control of cyclic movements using functional neuromuscular stimulation," *IEEE Trans. Rehab. Eng.*, vol. 8, pp. 42–52, Mar. 2000.

[13] E. C. Stites and J. J. Abbas, "Sensitivity and versatility of an adaptive system for controlling cyclic movements using functional neuromuscular stimulation," *IEEE Trans. Biomed. Eng.*, vol. 47, pp. 1287–1292, Sept. 2000.

[14] M. Ferrarin and A. Pedotti, "The relationship between electrical stimulus and joint torque: A dynamic model," *IEEE Trans. Rehab. Eng.*, vol. 8, pp. 342–352, Sept. 2000.

[15] R. B. Stein, E. P. Zehr, M. K. Lebiedowska, D. B. Popovic, A. Scheiner, and H. J. Chizeck, "Estimating mechanical parameters of leg segments in individuals with and without physical disabilities," *IEEE Trans. Rehab. Eng.*, vol. 4, pp. 201–211, Sept. 1996.

[16] J. P. Holden and S. J. Stanhope, "The effect of variation in knee center location estimates on net knee joint moments," *Gait Posture*, vol. 7, pp. 1–6, 1998.

[17] F. E. Zajac, "Muscle and tendon properties: Models, scaling, and application to biomechanics and motor control," *CRC Critical Rev. Biomed. Eng.*, vol. 17, pp. 359–411, 1989.

[18] R. Riener, M. Ferrarin, E. E. Pavan, and C. Frigo, "Patient-driven control of FES-supported standing up and sitting down: Experimental results," *IEEE Trans. Rehab. Eng.*, vol. 8, pp. 523–529, Dec. 2000.

[19] H. Hatze, "A comprehensive model of human motion simulation and its application to the take off phase of the long jump," *J. Biomech.*, vol. 14, pp. 135–142, 1981.

[20] J. M. Winters, "Hill-based muscle models: a system engineering perspective," in *Multiple Muscle Systems*, J. Winters and S. Woo, Eds. New York: Springer-Verlag, 1990, pp. 69–93.

[21] J. M. Winters and L. Stark, "Analysis of fundamental movement patterns through the use of in-depth antagonistic muscle models," *IEEE Trans. Biomed. Eng.*, vol. BE-32, pp. 826–839, 1985.

[22] R. Riener and T. Edrich, "Identification of passive elastic joint moments in the lower extremities," *J. Biomech.*, vol. 32, no. 5, pp. 539–544, 1999.

[23] T. Edrich, R. Riener, and J. Quintern, "Analysis of passive elastic joint moments of the lower extremities in paraplegics and normal controls," *IEEE Trans. Biomed. Eng.*, vol. 47, pp. 1058–1065, Aug. 2000.

[24] V. M. Zatsiorsky and V. Seluyanov, "The mass and inertia characteristics of the main segments of human body," in *Biomechanics VIII-B*, H. Matsui and K. Kobayashi, Eds. Champaign, IL: Human Kinetics, 1983, pp. 1152–1159.

[25] R. Riener and T. Fuhr, "Patient-driven control of FES-supported standing up: A simulation study," *IEEE Trans. Rehab. Eng.*, vol. 6, pp. 113–124, June 1998.

[26] M. Ferrarin, P. Iacuone, A. Mingrino, C. Frigo, and A. Pedotti, "A dynamic model of electrically activated knee muscles in healthy and paraplegics," in *Neuroprosthetics from Basic Research to Clinical Applications*, A. Pedotti, M. Ferrarin, R. Riener, and J. Quintern, Eds. Berlin, Germany: Springer-Verlag, 1996, pp. 81–90.

[27] I. Bar-Kana and H. Kaufman, "Simple adaptive control of uncertain systems," *Int. J. Adaptive Contr. Signal Processing*, vol. 2, pp. 133–143, 1988.

[28] K. Y. Tong and M. H. Granat, "Gait-control system for functional electrical stimulation using neural networks," *Med. Biol. Eng. Comput.*, vol. 37, pp. 35–41, 1999.

[29] S. Jonic, T. Jankovic, T. Gajic, and D. Popovic, "Three machine learning techniques for automatic determination of rules to control locomotion," *IEEE Trans. Biomed. Eng.*, vol. 46, pp. 300–310, 1999.

[30] D. Graupe and H. Kordylewski, "Artificial neural network control of FES in paraplegics for patient responsive ambulation," *IEEE Trans. Biomed. Eng.*, vol. 42, pp. 699–707, July 1995.

[31] A. Kostov, B. Andrews, D. Popovic, R. Stein, and W. Armstrong, "Machine learning in control of functional electrical stimulation systems for locomotion," *IEEE Trans. Biomed. Eng.*, vol. 42, pp. 541–551, June 1995.

[32] R. Davoodi and B. J. Andrews, "Computer simulation of FES standing up in paraplegia: a self-adaptive fuzzy controller with reinforcement learning," *IEEE Trans. Rehab. Eng.*, vol. 6, pp. 151–161, June 1998.

[33] J.-J. Chen, N.-Y. Yu, D.-G. Huang, B. T. Ann, and G.-C. Chang, "Applying fuzzy logic to control cycling movement induced by functional electrical stimulation," *IEEE Trans. Rehab. Eng.*, vol. 5, pp. 158–169, June 1997.

[34] J. Quintern, F. Palazzo, R. Riener, T. Edrich, and M. Ferrarin, "Dynamic neuromuscular and stretch reflex model for FES control," in *Proc. 4th Int. Congress Neuromodulation Society*, Lucerne, Switzerland, 1998, p. 164.

[35] F. Bahrami, R. Riener, M. Buss, and G. Schmidt, "Optimal trajectory generation for a paraplegic patient rising from a chair by means of FES," in *Neuroprosthetics from Basic Research to Clinical Applications*, A. Pedotti, M. Ferrarin, R. Riener, and J. Quintern, Eds. Berlin, Germany: Springer-Verlag, 1996, pp. 285–292.

[36] L. S. Chou, S. M. Song, and L. F. Draganich, "Predicting the kinematics of gait based on the optimum trajectory of the swing limb," *J. Biomech.*, vol. 28, pp. 377–385, 1995.

Maurizio Ferrarin (M'97) was born in Milan, Italy, in 1964. He received the M.Sc. degree in electronic engineering and the Ph.D. degree in bioengineering, both from the Polytechnic of Milan, Italy, in 1989 and 1993, respectively.

He is a Researcher with the Bioengineering Centre, Fnd. Don Carlo Gnocchi IRCCS ONLUS and Polytechnic of Milan, Milan, Italy, where he is responsible for the Laboratory for the Study of Motor Recovery (LaRMo). He is also a temporary Professor of Rehabilitation Robotics at the Polytechnic of Milan. His main research interests include FES and innovative orthosis, natural and artificial motor control, clinical gait analysis, biomechanics, visuospatial coordination, spasticity evaluation, and ergonomics of wheelchair propulsion and of seat cushions.

Dr. Ferrarin is a member of the IEEE Engineering in Medicine and Biology Society (IEEE/EMBS), the International Functional Electrical Stimulation Society (IFESS), and the Italian Society of Clinical Movement Analysis (SIAMoC).

Francesco Palazzo received the M.Sc. degree in electrical engineering from the Polytechnic of Milan, Italy, in 1998.

In 1997, he spent a semester at Queens University, Kingston, ON, Canada, working in the FES Research Group. In 1998, he spent a semester in the Automatic Control Department, Technical University of Munich, Germany. After almost two years spent in the field of information technology, his current interests and activities are in the field of medical imaging and diagnostic at General Electric Medical Systems, Paris, France.

Robert Riener (S'96–A'97–M'99) was born in Munich, Germany, in 1968. He received the Dipl.Ing. degree in mechanical engineering and the Dr. degree in engineering, both from the Technical University of Munich, Munich, in 1993 and 1997, respectively.

He spent time at the University of Maryland, Baltimore, as a Prof. Erich Müller Stiftung Scholar in 1993. In 1993, he joined the Institute of Automatic Control Engineering, Technical University of Munich, where he has pursued research into modeling and control of neuroprostheses. After postdoctoral work at the Centro di Bioingegneria, Politecnico di Milano, Milan, Italy, from 1998 to 1999, he returned to the Institute of Automatic Control Engineering, where he works on his habilitation about virtual reality technologies applied to medicine. He is responsible for several national and international research projects. His research interests involve control of normal and pathological limb movements, neuroprosthetics, biomechanical modeling, movement analysis, and virtual reality with haptic feedback.

Dr. Riener is a member of the IEEE Engineering in Medicine and Biology Society (IEEE/EMBS) and a founding member of the International Functional Electrical Stimulation Society (IFESS).

Jochen Quintern received the M.D. degree in 1983 with a dissertation on muscle tone in spasticity and rigidity.

Since 1989, he has been with the Department of Neurology, University of Munich, Munich, Germany, with a specialty in neurology. From 1983 to 1986, he was a Research Associate with the University of Freiburg, Germany. From 1986 to 1987, he was a Senior Research Associate with the Pritzker Institute of Medical Engineering, IIT, Chicago, IL. From 1987 to 1989, he was a lecturer with the German Sports College, Cologne, Germany, in the field of neurologic rehabilitation. He is a Project Leader for the development and application of neural prostheses for stance and gait. Since March 2000, he has been a consultant to the Neurological Hospital Bad Aibling, Germany. His scientific interests include natural and artificial motor control, spinal cord physiology and pathophysiology, and rehabilitation after upper motor neuron lesions.